



HAL
open science

Isospin amplitudes in $\Lambda_b^0 \rightarrow J/\psi\Lambda(\Sigma^0)$ and $\Xi_b^0 \rightarrow J/\psi\Xi^0(\Lambda)$ decays

Roel Aaij, Carlos Abellán Beteta, Thomas Ackernley, Bernardo Adeva, Marco Adinolfi, Hossein Afsharnia, Christine Angela Aidala, Salvatore Aiola, Ziad Ajaltouni, Simon Akar, et al.

► To cite this version:

Roel Aaij, Carlos Abellán Beteta, Thomas Ackernley, Bernardo Adeva, Marco Adinolfi, et al.. Isospin amplitudes in $\Lambda_b^0 \rightarrow J/\psi\Lambda(\Sigma^0)$ and $\Xi_b^0 \rightarrow J/\psi\Xi^0(\Lambda)$ decays. *Phys.Rev.Lett.*, 2020, 124 (11), pp.111802. 10.1103/PhysRevLett.124.111802. hal-02409865

HAL Id: hal-02409865

<https://hal.science/hal-02409865>

Submitted on 7 Sep 2023

HAL is a multi-disciplinary open access archive for the deposit and dissemination of scientific research documents, whether they are published or not. The documents may come from teaching and research institutions in France or abroad, or from public or private research centers.

L'archive ouverte pluridisciplinaire **HAL**, est destinée au dépôt et à la diffusion de documents scientifiques de niveau recherche, publiés ou non, émanant des établissements d'enseignement et de recherche français ou étrangers, des laboratoires publics ou privés.



Isospin amplitudes in $\Lambda_b^0 \rightarrow J/\psi \Lambda(\Sigma^0)$ and $\Xi_b^0 \rightarrow J/\psi \Xi^0(\Lambda)$ decays

LHCb collaboration[†]

Abstract

Ratios of isospin amplitudes in hadron decays are a useful probe of the interplay between weak and strong interactions, and allow searches for physics beyond the Standard Model. We present the first results on isospin amplitudes in b -baryon decays, using data corresponding to an integrated luminosity of 8.5 fb^{-1} , collected with the LHCb detector in pp collisions at center of mass energies of 7, 8 and 13 TeV. The isospin amplitude ratio $|A_1(\Lambda_b^0 \rightarrow J/\psi \Sigma^0)/A_0(\Lambda_b^0 \rightarrow J/\psi \Lambda)|$, where the subscript on A indicates the final-state isospin, is measured to be less than $1/21.8$ at 95% confidence level. The Cabibbo suppressed $\Xi_b^0 \rightarrow J/\psi \Lambda$ decay is observed for the first time, allowing for the measurement $|A_0(\Xi_b^0 \rightarrow J/\psi \Lambda)/A_{1/2}(\Xi_b^0 \rightarrow J/\psi \Xi^0)| = 0.37 \pm 0.06 \pm 0.02$, where the uncertainties are statistical and systematic, respectively.

Published in Physical Review Letters 124 (2020) 111802

© 2020 CERN for the benefit of the LHCb collaboration. CC-BY-4.0 licence.

[†]Authors are listed at the end of this paper.

Measurements of ratios of isospin amplitudes A_i (i denotes the final state isospin) in hadronic weak decays are a sensitive way to probe the interplay between strong and weak interactions. Such ratios can also reveal the presence of non-Standard Model amplitudes. For example, in $K \rightarrow \pi\pi$ decays the experimentally determined ratio $|A_0/A_2| \approx 22.5$ has not been understood for over 50 years [1]. Recent models of the strong dynamics [2] and lattice gauge calculations [3] for these decays give only partial explanations. Determinations of isospin amplitudes from $D \rightarrow \pi\pi$ and $B \rightarrow \pi\pi$ decays, using input from other two-body decays into light hadrons, found $|A_0/A_2| \approx 2.5$ [4], and $|A_0/A_2| \approx 1.0$ [5], respectively.

In this Letter, we investigate $\Lambda_b^0 \rightarrow J/\psi \Lambda(\Sigma^0)$ and $\Xi_b^0 \rightarrow J/\psi \Xi^0(\Lambda)$ decays. (Mention of a specific decay implies the use of its charge-conjugate as well.) The leading order Feynman diagrams for all four processes are shown in Fig. 1. The isospins of the J/ψ meson and Λ baryon are zero, and that of the Σ^0 baryon is one. The isospin of the Λ_b^0 baryon is predicted by the quark model to be zero. Since the $b \rightarrow c\bar{c}s$ weak operator involves no isospin change, if this prediction is correct, we expect a dominant A_0 amplitude and a preference for the $J/\psi \Lambda$ final state over $J/\psi \Sigma^0$, which proceeds via the A_1 amplitude. Isospin breaking effects are possible due to the difference in mass and charge of the u and d quarks and can also be induced by QED, electroweak-penguin, or new physics processes [6]. If the Λ_b^0 baryon comprises a ud diquark such effects should be small. Mixing of the Λ and Σ^0 baryons is also predicted to be small, $\sim 1^\circ$, and could contribute ~ 0.01 to the $|A_1/A_0|$ amplitude ratio [7]. A severely suppressed $J/\psi \Sigma^0$ final state would determine the isospin of the Λ_b^0 baryon to be zero. Some previous LHCb analyses of Λ_b^0 decays made assumptions concerning isospin amplitudes. For instance, the pentaquark analysis, using the $\Lambda_b^0 \rightarrow J/\psi K^- p$ channel [8], assumed that the A_0 amplitude was dominant, and in the measurement of $|V_{ub}/V_{cb}|$ using $\Lambda_b^0 \rightarrow p \mu^- \bar{\nu}$ decays [9] the $A_{3/2}$ amplitude was assumed to be much smaller than the $A_{1/2}$ amplitude.

In $\Xi_b^0 \rightarrow J/\psi \Xi^0(\Lambda)$ decays, taking the Ξ_b isospin as $1/2$, the final state results from an isospin change of zero ($1/2$) and has $A_i = A_{1/2}$ (A_0). In the reaction resulting in a final state Λ baryon, the weak transition changes isospin due to the $b \rightarrow c\bar{c}d$ rather than the $b \rightarrow c\bar{c}s$ transition. Here we investigate if the larger isospin change is suppressed, or if the decay amplitude is independent of the isospin change. Note that we measure the decay $\Xi_b^- \rightarrow J/\psi \Xi^-$ for two purposes: as a proxy for $\Xi_b^0 \rightarrow J/\psi \Xi^0$, which is difficult for us to measure, and to determine the background in $J/\psi \Lambda$ mass spectrum from these decays where $\Xi \rightarrow \Lambda\pi$.

The LHCb detector is a single-arm forward spectrometer covering the pseudorapidity range $2 < \eta < 5$, described in detail in Refs. [10, 11]. The trigger [12] consists of a hardware stage, based on information from the calorimeter and muon systems, followed by a software stage, which reconstructs charged particles. Natural units are used here with $c = \hbar = 1$. We use data collected by the LHCb detector, corresponding to 1.0 fb^{-1} of integrated luminosity in 7 TeV pp collisions, 2.0 fb^{-1} at 8 TeV, and 5.5 fb^{-1} collected at

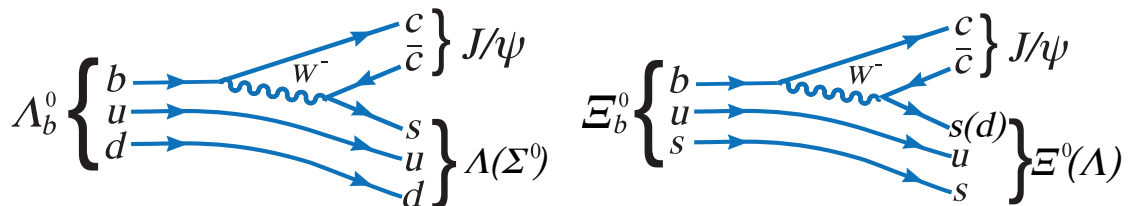


Figure 1: Leading order Feynman diagrams for $\Lambda_b^0 \rightarrow J/\psi \Lambda(\Sigma^0)$ and $\Xi_b^0 \rightarrow J/\psi \Xi^0(\Lambda)$ decays.

13 TeV. Hereafter, the data recorded at 7 and 8 TeV is referred to as Run 1 and the data recorded at 13 TeV is referred to as Run 2.

Simulation is required to model the effects of the detector acceptance and selection requirements. We generate pp collisions using PYTHIA [13] with a specific LHCb configuration [14]. Decays of unstable particles are described by EVTGEN [15], where final-state radiation is generated using PHOTOS [16]. The interaction of the particles with the detector, and its response, are implemented using the GEANT4 toolkit [17] as described in Ref. [18]. The lifetimes for the Λ_b^0 and Ξ_b^- baryons are taken as 1.473 and 1.572 ps [19], respectively. All simulations are performed separately for Run 1 and Run 2.

Our strategy is to fully reconstruct the $J/\psi\Lambda$ final state and partially reconstruct the $J/\psi\Sigma^0$ mode by ignoring the photon from the $\Sigma^0 \rightarrow \gamma\Lambda$ decay, because of the low efficiency of the calorimeter at small photon energies. For these decays the $J/\psi\Lambda$ mass distribution is almost uniform in the mass range 5350–5620 MeV. We simulate its shape and then fit the mass distribution to ascertain its size. The J/ψ meson is reconstructed through the $J/\psi \rightarrow \mu^+\mu^-$ decay. Candidates are formed by combining two oppositely charged tracks identified as muons, with transverse momentum $p_T > 550$ MeV. Each of the two muons are required to have a maximal χ^2 of distance of closest approach of 30 and are also required to form a vertex with $\chi_{\text{vtx}}^2 < 16$. The J/ψ candidate is required to have a decay length significance from every primary vertex, PV, of greater than 3 and a mass in the range 3049–3140 MeV.

Candidate Λ baryons are formed from a pair of identified proton and π^- particles, each with momentum greater than 2 GeV. Due to their long lifetime and high boost, a majority of the Λ baryons decay after the vertex detector. However, we use only putative decays that occur inside the vertex detector. Each of the two tracks must be inconsistent with having originated from a PV, have a maximal χ^2 of distance of closest approach of 30, form a vertex with $\chi_{\text{vtx}}^2 < 12$ that is separated from that PV by more than 3 standard deviations, and have a mass between 1105 and 1124 MeV. In addition, we eliminate candidates that when interpreted as $\pi^+\pi^-$ fall within 7.5 MeV of the known K_S^0 mass. Candidate $\Xi^- \rightarrow \Lambda\pi^-$ decays are reconstructed using the criteria in Ref. [20], with the additional requirement that the Ξ^- decays in the LHCb vertex detector. These are combined with selected J/ψ mesons to form candidate Ξ_b^- baryons.

We improve the $J/\psi\Lambda$ mass resolution by constraining the J/ψ and Λ candidates to their known masses and their decay products to originate from each of the relevant decay vertices; we also constrain the J/ψ and the Λ candidates to come from the same decay point [21].

After these selections, we use two boosted decision trees (BDT) [22, 23] implemented in the TMVA toolkit [24] to further separate signal from background. The first BDT is trained to reject generic $b \rightarrow J/\psi X$ decays where X contains one or more charged tracks. We train this “isolation” BDT using the following information: the χ_{IP}^2 of additional charged tracks with respect to the J/ψ vertex, where χ_{IP}^2 is defined as the difference in the χ_{vtx}^2 of the J/ψ vertex reconstructed with and without the track being considered; the χ_{vtx}^2 of the vertex formed by the J/ψ plus each additional track; the minimum χ_{IP}^2 of the additional track with respect to any PV; and the p_T of the additional track. For the isolation BDT training, we use samples of $\Lambda_b^0 \rightarrow J/\psi\Lambda$ and $B^- \rightarrow J/\psi K^-$ candidates for the signal and background models, respectively. Both samples are background subtracted using the *sPlot* technique [25]. The output of the isolation BDT is used as an input variable in the final BDT.

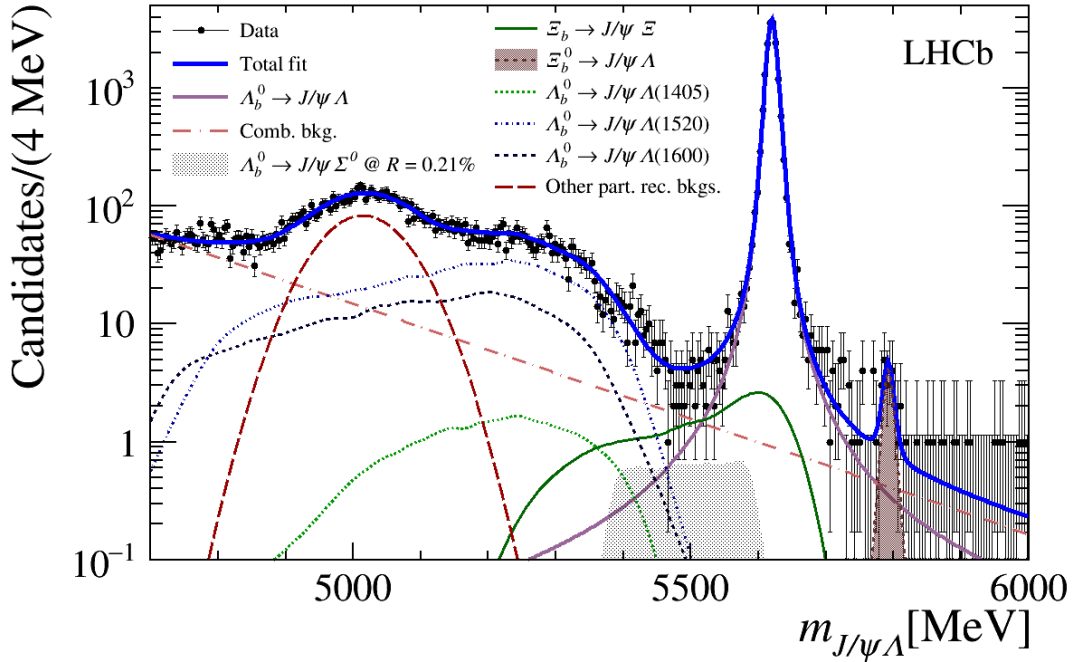


Figure 2: Distribution of the $J/\psi\Lambda$ mass for Run 2 data. Error bars without data points indicate empty bins. Also shown is the projection of the joint fit to the data. The thick (blue) solid curve shows the total fit. For illustrative purposes, the $\Lambda_b^0 \rightarrow J/\psi\Sigma^0$ signal component is artificially scaled to its measured upper limit. The shapes are identified in the legend.

The twenty discrimination variables used in the final BDT are listed in the Supplemental material. These mostly exploit the topology of the decay using the vertexing properties of the J/ψ , Λ , and Λ_b^0 candidates, and particle identification of their decay products. The signal sample again is background-subtracted $\Lambda_b^0 \rightarrow J/\psi\Lambda$ combinations. For background training we use candidates in the upper sideband with $J/\psi\Lambda$ masses between 5.7–6.0 GeV, excluding events in 5.77–5.81 GeV to avoid including $\Xi_b^0 \rightarrow J/\psi\Lambda$ decays in the background sample. We use k-folding cross validation with five folds in both BDTs, to avoid any possible bias [26]. The final BDT selection is optimized to maximize the Punzi figure of merit, $\epsilon_s/(\sqrt{B} + 1.5)$ [27], where ϵ_s is the efficiency of the final BDT selection on simulated $\Lambda_b^0 \rightarrow J/\psi\Sigma^0$ decays and B is the number of background candidates in the above defined sideband that pass the BDT requirement, scaled to the width of the $J/\psi\Sigma^0$ signal window. The analysis is performed separately on Run 1 and Run 2 data. The resulting $J/\psi\Lambda$ mass spectrum for Run 2 data is shown in Fig. 2. The Run 1 mass distribution is similar and is shown in the Supplemental material.

There are two signal peaks evident in the mass distribution in Fig. 2. The larger is due to $\Lambda_b^0 \rightarrow J/\psi\Lambda$ decays, and the smaller corresponds to $\Xi_b^0 \rightarrow J/\psi\Lambda$ decays. The latter is a heretofore unobserved Cabibbo-suppressed decay. The Run 1 and 2 mass distribution data are fit jointly to determine the $\Lambda_b^0 \rightarrow J/\psi\Lambda$, $\Lambda_b^0 \rightarrow J/\psi\Sigma^0$ and $\Xi_b^0 \rightarrow J/\psi\Lambda$ yields. The $\Lambda_b^0 \rightarrow J/\psi\Sigma^0$ signal is modeled using a Gaussian kernel [28] shape fit to simulation. The $\Lambda_b^0 \rightarrow J/\psi\Lambda$ signal is described by a Hypatia function, whose tail parameters are fixed from simulation, with the mass and width allowed to vary in the fit to the data. [29]. The $\Xi_b^0 \rightarrow J/\psi\Lambda$ peak is fit to the same shape but with its mean constrained to the fitted Λ_b^0

mass plus the known $\Xi_b^0 - \Lambda_b^0$ mass difference of 172.5 MeV [19].

While most of the candidates above the Λ_b^0 peak are the result of combinatoric background, those below are due to additional sources. One is due to $\Lambda_b^0 \rightarrow J/\psi \Lambda^*$ decays, with $\Lambda^* \rightarrow \Sigma^0 \pi^0$ and $\Sigma^0 \rightarrow \gamma \Lambda$. Here, Λ^* denotes strange-baryon resonances ranging from 1405 MeV to 2350 MeV in mass. Another source comprises partially reconstructed $\Lambda_b^0 \rightarrow \psi(2S) \Lambda$ decays, where $\psi(2S) \rightarrow \pi \pi J/\psi$. These decays mainly populate masses lower than the $\Lambda_b^0 \rightarrow J/\psi \Sigma^0$ signal, but need to be included to accurately model the combinatoric background. The existence of the $\Lambda_b^0 \rightarrow J/\psi \Lambda^*$ channels was demonstrated in a study of $\Lambda_b^0 \rightarrow J/\psi K^- p$ decays [8]. We can model the resulting $J/\psi \Lambda$ mass shapes of the different $\Lambda_b^0 \rightarrow J/\psi \Lambda^*$ backgrounds, although we do not know their yields due to lack of knowledge of the relative $\Lambda^* \rightarrow \Sigma^0 \pi^0$ branching fractions. We use separate shapes in the fit for the backgrounds corresponding to the $\Lambda(1405)$, $\Lambda(1520)$ and $\Lambda(1600)$ resonances. These backgrounds are simulated, processed through the event selections and fit using Gaussian kernel shapes. We collectively model the sum of the remaining Λ^* and $\psi(2S)$ backgrounds in the fit using a Gaussian shape. Note that our aim here is not to accurately disentangle each source of background, but only to model their collective sum.

A third background source arises from $\Xi_b \rightarrow J/\psi \Xi$ decays, where $\Xi \rightarrow \Lambda \pi$, when the pion from the Ξ decay is not reconstructed. This background is modeled by a Gaussian kernel shape fit to simulated $\Xi_b^- \rightarrow J/\psi \Xi^-$ decays, which are partially reconstructed as $J/\psi \Lambda$. The normalization of this background is determined by fully reconstructing $\Xi_b^- \rightarrow J/\psi \Xi^-$ decays in data and simulation to obtain an efficiency-corrected yield. The reconstruction uses the criteria in Ref. [20]. The reconstructed $J/\psi \Xi^-$ mass distribution in data is shown in the Supplemental material. The efficiency-corrected yield is multiplied by the relative efficiency of reconstructing $\Xi_b^- \rightarrow J/\psi \Xi^-$, as $J/\psi \Lambda$, and then more than doubled to account for $\Xi_b^0 \rightarrow J/\psi \Xi^0$ decays. The production rates are unequal mostly because the $\Xi_b'(5935)^0$ state is too light to decay into $\Xi_b^- \pi^+$ so it always decays into the Ξ_b^0 baryon [30]. In addition, we incorporate the production measurements of other excited Ξ_b resonances [31] to determine the inclusive production ratio of $\Xi_b^0/\Xi_b^- = 1.37 \pm 0.09$, where the uncertainty arises mainly from the production fraction measurements of the excited states. We further corrected for the lifetime ratio $\tau_{\Xi_b^-}/\tau_{\Xi_b^0} = 1.08 \pm 0.04$ [32]. This normalization is introduced into the final fit as a Gaussian constraint, and done separately for Run 1 and Run 2 data, as the detection efficiencies differ.

The remaining background comes mostly from random combinations of real J/ψ and Λ , which contribute both above and below the $\Lambda_b^0 \rightarrow J/\psi \Lambda$ mass peak. This combinatoric background is modeled using an exponential function.

The Run 1 and Run 2 mass distribution data are fit simultaneously, using a binned extended maximum-likelihood fit, where the efficiency-corrected relative yields of the $\Lambda_b^0 \rightarrow J/\psi \Sigma^0$ signal, and those of the three $\Lambda_b^0 \rightarrow J/\psi \Lambda^*$ decays, with respect to the $\Lambda_b^0 \rightarrow J/\psi \Lambda$ signal, are constrained to be the same in the two data sets. We define

$$\mathcal{R} \equiv \frac{|A_1|^2}{|A_0|^2} = \frac{\mathcal{B}(\Lambda_b^0 \rightarrow J/\psi \Sigma^0)}{\mathcal{B}(\Lambda_b^0 \rightarrow J/\psi \Lambda)} \cdot \Phi_{\Lambda_b^0} = \frac{N_{\Lambda_b^0 \rightarrow J/\psi \Sigma}}{N_{\Lambda_b^0 \rightarrow J/\psi \Lambda}} \cdot \frac{\epsilon_{\Lambda_b^0 \rightarrow J/\psi \Lambda}}{\epsilon_{\Lambda_b^0 \rightarrow J/\psi \Sigma}} \cdot \Phi_{\Lambda_b^0}, \quad (1)$$

where $N_{\Lambda_b^0 \rightarrow J/\psi \Sigma}$ and $N_{\Lambda_b^0 \rightarrow J/\psi \Lambda}$ are the yields of the $\Lambda_b^0 \rightarrow J/\psi \Sigma$ and $\Lambda_b^0 \rightarrow J/\psi \Lambda$ decays; $\epsilon_{\Lambda_b^0 \rightarrow J/\psi \Sigma}$ and $\epsilon_{\Lambda_b^0 \rightarrow J/\psi \Lambda}$ are their respective efficiencies, as estimated from simulation; the phase space correction factor, $\Phi_{\Lambda_b^0}$, is 1.058. The free parameters of interest in the fit are \mathcal{R} , $N_{\Lambda_b^0 \rightarrow J/\psi \Lambda}$, and $N_{\Xi_b^0 \rightarrow J/\psi \Lambda}$; $N_{\Lambda_b^0 \rightarrow J/\psi \Sigma}$ can be calculated from these. Systematic

uncertainties are folded into the fit components as Gaussian constraints. These include uncertainties on the simulated ratios of efficiencies for the different Λ_b^0 final states with respect to the $J/\psi\Lambda$ final state, which range from 1.4 to 2.4%. The uncertainty on the relative normalization of the $\Xi_b \rightarrow J/\psi\Xi$ background is estimated to be 12.1% for Run 1 and 9.8% for Run 2. This has contributions from the fit yield of the fully reconstructed $\Xi_b^- \rightarrow J/\psi\Xi^-$ decay, the reconstruction and efficiency of finding the $\Xi^- \rightarrow \Lambda\pi^-$ decay, and the Ξ_b^-/Ξ_b^0 lifetime ratio.

The results of the fit are shown in Fig. 2, and reported in Table 1. The fitted value for \mathcal{R} , is consistent with zero. In Fig. 2, we illustrate what this component would look like if observed at the upper limit on \mathcal{R} . We do not quote the yields of the $\Lambda_b^0 \rightarrow J/\psi\Lambda^*$ decays as these are highly correlated.

To set an upper limit on \mathcal{R} we use the CLs method [33]. The variation of the observed and expected CLs versus \mathcal{R} is scanned from 0 to 0.005 and shown in Fig. 3. Our observed upper limit on \mathcal{R} is

$$\mathcal{R} < 0.0021 \text{ at } 95\% \text{ CL.}$$

Systematic uncertainties are incorporated in the fit and included in this limit. Further consistency checks include changing the fit range, eliminating the $\Lambda_b^0 \rightarrow J/\psi\Lambda^*$ background components one at a time, and fitting the $\Lambda_b^0 \rightarrow J/\psi\Lambda$ peak with different functions. These change the upper limit only by small amounts.

The Run 1 and Run 2 signal yields for $\Xi_b^0 \rightarrow J/\psi\Lambda$ are listed in Table 1. The statistical significance of the $\Xi_b^0 \rightarrow J/\psi\Lambda$ signal is 5.6 standard deviations, obtained using Wilks' theorem [34] and includes both the statistical and systematic uncertainties. The branching fraction ratio $\mathcal{B}(\Xi_b^0 \rightarrow J/\psi\Lambda)/\mathcal{B}(\Xi_b^0 \rightarrow J/\psi\Xi^0)$ is determined using the fully reconstructed $\Xi_b^- \rightarrow J/\psi\Xi^-$ sample described above. To determine the branching fraction of $\mathcal{B}(\Xi_b^0 \rightarrow J/\psi\Xi^0)$, we assume equal decay widths for the two different $\Xi_b \rightarrow J/\psi\Xi$ charge states and correct for the different neutral and charged Ξ_b production rates as described above. We use the measured lifetime ratio [32] to translate the decay width equality into the needed branching fraction. The Run 1 and Run 2 results are consistent. Combining the two, we find

$$R_{\Xi_b} \equiv \frac{\mathcal{B}(\Xi_b^0 \rightarrow J/\psi\Lambda)}{\mathcal{B}(\Xi_b^0 \rightarrow J/\psi\Xi^0)} = (8.2 \pm 2.1 \pm 0.9) \cdot 10^{-3},$$

where the first uncertainty is statistical the second is systematic, where the leading source is the systematic uncertainty in the $\Xi_b^- \rightarrow J/\psi\Xi^-$ fit yield.

Table 1: Results from the fit to the $J/\psi\Lambda$ mass distribution. The fitted yields are indicated by N . Note $N_{\Xi_b \rightarrow J/\psi\Xi}$ indicates the sum of Ξ_b^- and Ξ_b^0 decays.

Parameter	Shared value	Run 1 value	Run 2 value
\mathcal{R}	$(0 \pm 5.3) \cdot 10^{-4}$	–	–
$N_{\Lambda_b^0 \rightarrow J/\psi\Lambda}$	–	4417 ± 66	$16\,970 \pm 130$
$N_{\Xi_b \rightarrow J/\psi\Xi}$	–	23.3 ± 5.7	139.7 ± 21.9
$N_{\Xi_b^0 \rightarrow J/\psi\Lambda}$	–	6.2 ± 3.0	17.8 ± 5.1

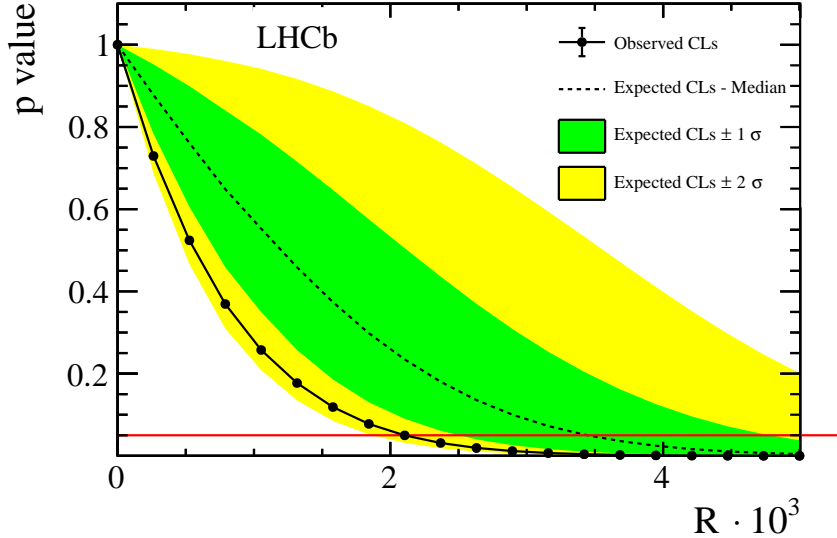


Figure 3: Result of the hypothesis tests conducted using the CLs method by varying \mathcal{R} is shown. The observed CLs distribution is shown by the round (black) points. The expected CLs distribution (based on the background only hypothesis) is shown by the dashed line (black), with 1 and 2 σ uncertainty bands depicted in dark shaded (green) and light shaded (yellow) bands. The observed and expected upper limits are obtained by seeing where the bands cross the p-value of 0.05 shown as the horizontal (red) line.

We convert R_{Ξ_b} into a measurement of the amplitude ratio

$$\left| \frac{A_0}{A_{1/2}} \right| = \frac{1}{\lambda} \sqrt{\frac{R_{\Xi_b}}{\Phi_{\Xi_b}}} = 0.37 \pm 0.06 \pm 0.02$$

where $\Phi_{\Xi_b} = 1.15$ is the relative phase space factor, and $\lambda = 0.231$ is the relative Cabibbo suppression $|V_{cd}|/|V_{cs}|$, which is assumed equal to $|V_{us}|/|V_{ud}|$ [19]. Taking the s and u quarks in the Ξ_b^0 baryon to be a diquark state with isospin 1/2 and combining with the null isospin of the s quark from the b quark decay, leads to isospin 1/2 for the $J/\psi \Xi^0$ final state. On the other hand, for the Cabibbo suppressed transition with the isospin 1/2 d quark, we have either isospin 0 or 1 final states. The former corresponds to $J/\psi \Lambda$, with the latter to $J/\psi \Sigma^0$, which we cannot currently measure. In order to predict the expected ratio of isospin amplitudes the SU(3) flavor [35] b -baryon couplings must be taken into account [36]. Then, if there are no other amplitudes, the theoretically predicted ratio corresponding to no preference between isospin 0 and 1/2 amplitudes is $|A_0/A_{1/2}|$ equal to $1/\sqrt{6}$ (≈ 0.41). Therefore, our result is consistent with no suppression of the isospin changing amplitude. These results are not precise enough to see the effects of SU(3) flavor symmetry breaking.

In conclusion, we set an upper limit in $\Lambda_b^0 \rightarrow J/\psi \Lambda(\Sigma^0)$ decays on the isospin amplitude ratio

$$|A_1/A_0| = \sqrt{\mathcal{R}} < 1/21.8 \text{ at } 95\% \text{ CL.}$$

This limit is stringent and rules out isospin violation at a $\sim 1\%$ rate. Isospin violation has been seen at this level, for example, in $\rho - \omega$ mixing in $\bar{B}^0 \rightarrow J/\psi \pi^+ \pi^-$ decays [37]. Our limit is consistent with the Λ_b^0 being formed of a b quark and a ud diquark. This

measurement also constrains non-Standard Model A_1 amplitudes contributing to Λ_b^0 decays. Furthermore, our results support the quark model prediction of the Λ_b^0 being an isosinglet. Assumptions of isospin suppression in $\Lambda_b^0 \rightarrow J/\psi X$ decays made in past analyses are shown to be justified. Finally, we report the discovery of the Cabibbo suppressed decay $\Xi_b^0 \rightarrow J/\psi \Lambda$ and measure its branching fraction relative to $\Xi_b^0 \rightarrow J/\psi \Xi^0$ to be $(8.2 \pm 2.1 \pm 0.9) \cdot 10^{-3}$. We see no evidence for the preference of either isospin amplitude in the ratio $|A_0/A_{1/2}| = 0.37 \pm 0.06 \pm 0.02$, as the prediction for the equality of isospin amplitudes is $1/\sqrt{6}$.

Acknowledgements

We express our gratitude to our colleagues in the CERN accelerator departments for the excellent performance of the LHC. We thank A. Ali, Y. Grossman, G. Isidori, Z. Ligeti, and J. Rosner for useful discussions. We thank the technical and administrative staff at the LHCb institutes. We acknowledge support from CERN and from the national agencies: CAPES, CNPq, FAPERJ and FINEP (Brazil); MOST and NSFC (China); CNRS/IN2P3 (France); BMBF, DFG and MPG (Germany); INFN (Italy); NWO (Netherlands); MNiSW and NCN (Poland); MEN/IFA (Romania); MSHE (Russia); MinECo (Spain); SNSF and SER (Switzerland); NASU (Ukraine); STFC (United Kingdom); DOE NP and NSF (USA). We acknowledge the computing resources that are provided by CERN, IN2P3 (France), KIT and DESY (Germany), INFN (Italy), SURF (Netherlands), PIC (Spain), GridPP (United Kingdom), RRCKI and Yandex LLC (Russia), CSCS (Switzerland), IFIN-HH (Romania), CBPF (Brazil), PL-GRID (Poland) and OSC (USA). We are indebted to the communities behind the multiple open-source software packages on which we depend. Individual groups or members have received support from AvH Foundation (Germany); EPLANET, Marie Skłodowska-Curie Actions and ERC (European Union); ANR, Labex P2IO and OCEVU, and Région Auvergne-Rhône-Alpes (France); Key Research Program of Frontier Sciences of CAS, CAS PIFI, and the Thousand Talents Program (China); RFBR, RSF and Yandex LLC (Russia); GVA, XuntaGal and GENCAT (Spain); the Royal Society and the Leverhulme Trust (United Kingdom).

A Supplemental material

The material here comprises the main BDT input variables in Section A.1, the projection of the fit to the Run 1 $J/\psi\Lambda$ mass spectrum in Section A.2, and the fits to the $J/\psi\Xi^-$ mass spectra in Section A.3.

A.1 Final BDT variables

The variables used to train the BDT are:

1. The χ^2 of the global fit done by constraining the masses of the J/ψ and Λ particles to their known values and their momenta to the point of common origin.
2. The minimum χ_{IP}^2 of the Λ_b^0 candidate with respect to all the PVs.
3. The DIRA of the Λ_b^0 candidate with respect to its best PV, where DIRA of a particle is defined as its displacement vector with respect to the vertex.
4. The significance of the flight distance of the Λ_b^0 candidate with respect to the best PV.
5. The minimum χ_{IP}^2 of the J/ψ candidate with respect to all the PVs.
6. The mass of the two muons forming the J/ψ candidate.
7. The significance of the Λ candidates flight distance with respect to the J/ψ vertex.
8. The DIRA of the Λ candidate with respect to to the J/ψ vertex.
9. The flight distance of the Λ candidate with respect to to the J/ψ vertex.
10. The DIRA of the Λ candidate with respect to the best PV.
11. The absolute difference between the mass of the Λ candidate and its known value.
12. The minimum χ_{IP}^2 of the Λ candidate with respect to all the PVs.
13. The minimum χ_{IP}^2 of the proton with respect to all the PVs.
14. The probability that the proton from the Λ candidate is not a real track, called a “ghost.”
15. The p_{T} of the proton from the Λ decay.
16. The particle identification of the proton from the Λ decay.
17. The ghost probability of the pion from the Λ decay.
18. The minimum χ_{IP}^2 of the pion from the Λ decay with respect to all the PVs.
19. The p_{T} of the pion from the Λ decay.
20. Output of the isolation BDT.

A.2 Projection of the overall fit to the $J/\psi\Lambda$ mass spectrum in the Run 1 data

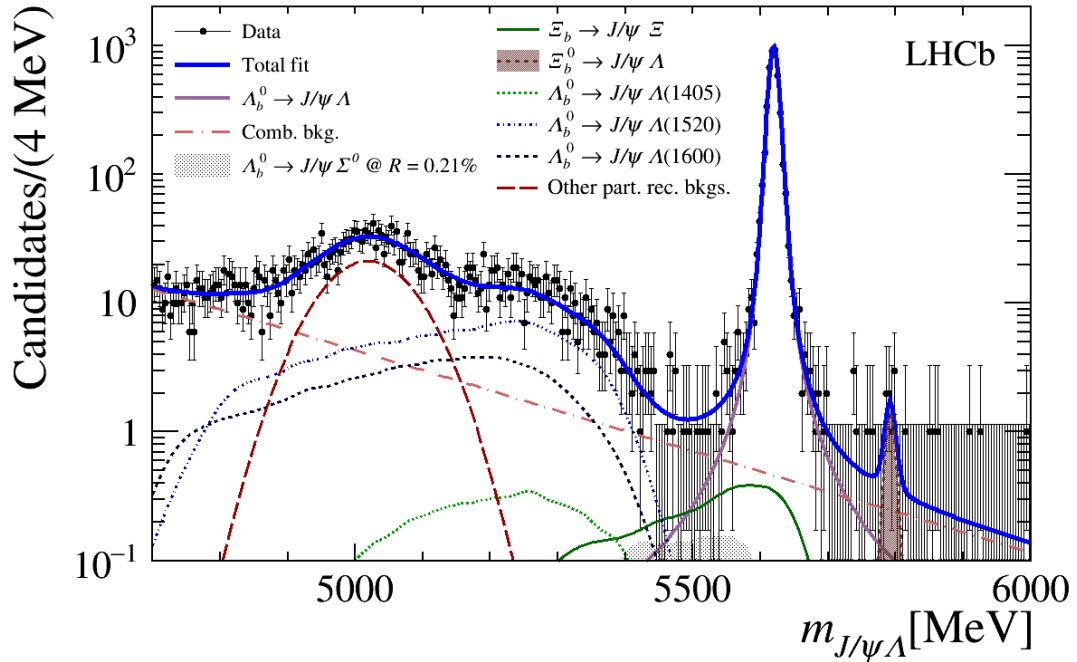


Figure 4: Distribution of $J/\psi\Lambda$ mass for Run 1 data. Error bars without data points indicate empty bins. Also shown is the projection of the joint fit to the data. The thick (blue) solid curve shows the total fit. The $\Lambda_b^0 \rightarrow J/\psi\Sigma^0$ signal component is artificially scaled to its measured upper limit. The rest of the shapes are identified in the legend.

A.3 Fits to the $J/\psi\Xi^-$ mass spectrum

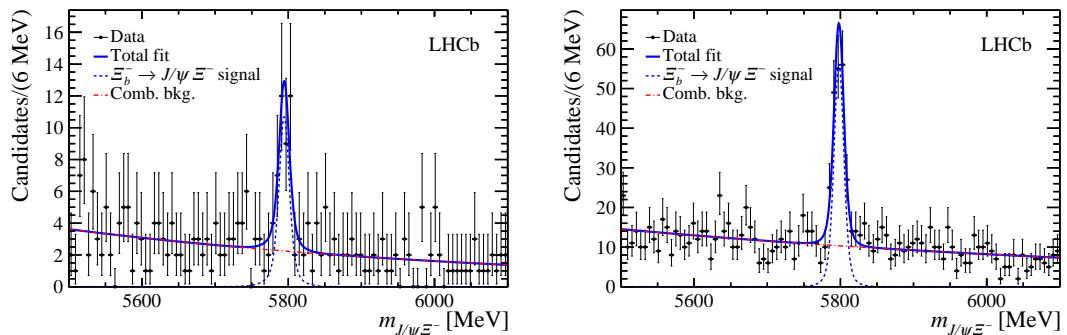


Figure 5: Distributions of $J/\psi\Xi^-$ mass shown as points with error bars for (left) Run 1 and (right) Run 2 data. The total fit to data is shown as a solid (blue) curve. The $\Xi_b^- \rightarrow J/\psi\Xi^-$ signal is fit with the sum of two Crystal Ball functions with the same mean and width, but different tail parameters, shown as the dashed (blue) curve. The combinatorial background shape is fit with an exponential function, shown as a dashed (red) curve.

References

- [1] H.-Y. Cheng, *Status of the $\Delta I = 1/2$ rule in kaon decay*, Int. J. Mod. Phys. **A4** (1989) 495.
- [2] A. J. Buras, J.-M. Gérard, and W. A. Bardeen, *Large N approach to kaon decays and mixing 28 years later: $\Delta I = 1/2$ Rule, \hat{B}_K and ΔM_K* , Eur. Phys. J. **C74** (2014) 2871, [arXiv:1401.1385](#).
- [3] RBC and UKQCD collaborations, P. A. Boyle *et al.*, *Emerging understanding of the $\Delta I = 1/2$ rule from lattice QCD*, Phys. Rev. Lett. **110** (2013) 152001, [arXiv:1212.1474](#); T. Blum *et al.*, *$K \rightarrow \pi\pi$ $\Delta I = 3/2$ decay amplitude in the continuum limit*, Phys. Rev. **D91** (2015) 074502, [arXiv:1502.00263](#); N. Ishizuka, K.-I. Ishikawa, A. Ukawa, and T. Yoshié, *Calculation of $K \rightarrow \pi\pi$ decay amplitudes with improved Wilson fermion action in lattice QCD*, Phys. Rev. **D92** (2015) 074503, [arXiv:1505.05289](#).
- [4] E. Franco, S. Mishima, and L. Silvestrini, *The Standard Model confronts CP violation in $D^0 \rightarrow \pi^+\pi^-$ and $D^0 \rightarrow K^+K^-$* , JHEP **05** (2012) 140, [arXiv:1203.3131](#).
- [5] B. Grinstein, D. Piratskhalava, D. Stone, and P. Uttayarat, *B decays to two pseudoscalars and a generalized $\Delta I = \frac{1}{2}$ rule*, Phys. Rev. **D89** (2014) 114014, [arXiv:1402.1164](#).
- [6] Y. Grossman, M. Neubert, and A. L. Kagan, *Trojan penguins and isospin violation in hadronic B decays*, JHEP **10** (1999) 029, [arXiv:hep-ph/9909297](#).
- [7] S. R. Coleman and S. L. Glashow, *Electrodynamical properties of baryons in the unitary symmetry scheme*, Phys. Rev. Lett. **6** (1961) 423; R. H. Dalitz and F. Von Hippel, *Electromagnetic $\Lambda - \Sigma^0$ mixing and charge symmetry for the Λ -hyperon*, Phys. Lett. **10** (1964) 153; CSSM/QCDSF/UKQCD collaboration, Z. R. Kordov *et al.*, *Electromagnetic contribution to Σ - Λ mixing using lattice QCD+QED*, [arXiv:1911.02186](#).
- [8] LHCb collaboration, R. Aaij *et al.*, *Observation of $J/\psi p$ resonances consistent with pentaquark states in $\Lambda_b^0 \rightarrow J/\psi K^- p$ decays*, Phys. Rev. Lett. **115** (2015) 072001, [arXiv:1507.03414](#).
- [9] LHCb collaboration, R. Aaij *et al.*, *Determination of the quark coupling strength $|V_{ub}|$ using baryonic decays*, Nature Phys. **11** (2015) 743, [arXiv:1504.01568](#).
- [10] LHCb collaboration, A. A. Alves Jr. *et al.*, *The LHCb detector at the LHC*, JINST **3** (2008) S08005.
- [11] LHCb collaboration, R. Aaij *et al.*, *LHCb detector performance*, Int. J. Mod. Phys. **A30** (2015) 1530022, [arXiv:1412.6352](#).
- [12] R. Aaij *et al.*, *The LHCb trigger and its performance in 2011*, JINST **8** (2013) P04022, [arXiv:1211.3055](#).

- [13] T. Sjöstrand, S. Mrenna, and P. Skands, *A brief introduction to PYTHIA 8.1*, Comput. Phys. Commun. **178** (2008) 852, [arXiv:0710.3820](#); T. Sjostrand, S. Mrenna, and P. Z. Skands, *PYTHIA 6.4 Physics and Manual*, JHEP **0605** (2006) 026, [arXiv:hep-ph/0603175](#).
- [14] I. Belyaev *et al.*, *Handling of the generation of primary events in Gauss, the LHCb simulation framework*, J. Phys. Conf. Ser. **331** (2011) 032047.
- [15] D. J. Lange, *The EvtGen particle decay simulation package*, Nucl. Instrum. Meth. **A462** (2001) 152.
- [16] P. Golonka and Z. Was, *PHOTOS Monte Carlo: A precision tool for QED corrections in Z and W decays*, Eur. Phys. J. **C45** (2006) 97, [arXiv:hep-ph/0506026](#).
- [17] GEANT4 collaboration, J. Allison *et al.*, *Geant4 developments and applications*, IEEE Trans. Nucl. Sci. **53** (2006) 270; GEANT4 collaboration, S. Agostinelli *et al.*, *GEANT4: a simulation toolkit*, Nucl. Instrum. Meth. **A506** (2003) 250.
- [18] M. Clemencic *et al.*, *The LHCb simulation application, Gauss: Design, evolution and experience*, J. Phys. Conf. Ser. **331** (2011) 032023.
- [19] Particle Data Group, M. Tanabashi *et al.*, *Review of particle physics*, Phys. Rev. **D98** (2018) 030001, and 2019 update.
- [20] LHCb collaboration, R. Aaij *et al.*, *Measurement of the mass and production rate of Ξ_b^- baryons*, Phys. Rev. **D99** (2019) 052006, [arXiv:1901.07075](#).
- [21] W. D. Hulsbergen, *Decay chain fitting with a Kalman filter*, Nucl. Instrum. Meth. **A552** (2005) 566, [arXiv:physics/0503191](#).
- [22] L. Breiman, J. H. Friedman, R. A. Olshen, and C. J. Stone, *Classification and regression trees*, Wadsworth international group, Belmont, California, USA, 1984.
- [23] R. E. Schapire and Y. Freund, *A decision-theoretic generalization of on-line learning and an application to boosting*, Journal Computer and System Sciences **55** (1997) 119.
- [24] A. Hoecker *et al.*, *TMVA: Toolkit for Multivariate Data Analysis*, PoS **ACAT** (2007) 040, [arXiv:physics/0703039](#); J. Stelzer, A. Hocker, P. Speckmayer, and H. Voss, *Current developments in TMVA: An outlook to TMVA4*, PoS **ACAT08** (2008) 063.
- [25] M. Pivk and F. R. Le Diberder, *sPlot: A Statistical tool to unfold data distributions*, Nucl. Instrum. Meth. **A555** (2005) 356, [arXiv:physics/0402083](#).
- [26] A. Bagoly *et al.*, *Machine learning developments in ROOT*, J. Phys. Conf. Ser. **898** (2017) 072046.
- [27] G. Punzi, *Sensitivity of searches for new signals and its optimization*, eConf **C030908** (2003) MODT002, [arXiv:physics/0308063](#).
- [28] K. S. Cranmer, *Kernel estimation in high-energy physics*, Comput. Phys. Commun. **136** (2001) 198, [arXiv:hep-ex/0011057](#).

- [29] D. Martnez Santos and F. Dupertuis, *Mass distributions marginalized over per-event errors*, Nucl. Instrum. Meth. **A764** (2014) 150, [arXiv:1312.5000](#).
- [30] LHCb, R. Aaij *et al.*, *Observation of two new Ξ_b^- baryon resonances*, Phys. Rev. Lett. **114** (2015) 062004, [arXiv:1411.4849](#).
- [31] LHCb, R. Aaij *et al.*, *Measurement of the properties of the Ξ_b^{*0} baryon*, JHEP **05** (2016) 161, [arXiv:1604.03896](#).
- [32] LHCb collaboration, R. Aaij *et al.*, *Precision measurement of the mass and lifetime of the Ξ_b^- baryon*, Phys. Rev. Lett. **113** (2014) 242002, [arXiv:1409.8568](#).
- [33] A. L. Read, *Presentation of search results: The CL_s technique*, J. Phys. **G28** (2002) 2693.
- [34] S. S. Wilks, *The large-sample distribution of the likelihood ratio for testing composite hypotheses*, Ann. Math. Statist. **9** (1938) 60.
- [35] G. Hiller, M. Jung, and S. Schacht, *$SU(3)_F$ in nonleptonic charm decays*, PoS **EPS-HEP2013** (2013) 371, [arXiv:1311.3883](#).
- [36] A. Dery, M. Ghosh, Y. Grossman, and S. Schacht, *$SU(3)_F$ analysis for beauty baryon decays*, [arXiv:2001.05397](#).
- [37] LHCb collaboration, R. Aaij *et al.*, *Measurement of the CP-violating phase β in $\bar{B}^0 \rightarrow J/\psi\pi^+\pi^-$ decays and limits on penguin effects*, Phys. Lett. **B742** (2015) 38, [arXiv:1411.1634](#).

LHCb collaboration

R. Aaij³¹, C. Abellán Beteta⁴⁹, T. Ackernley⁵⁹, B. Adeva⁴⁵, M. Adinolfi⁵³, H. Afsharnia⁹, C.A. Aidala⁸⁰, S. Aiola²⁵, Z. Ajaltouni⁹, S. Akar⁶⁶, P. Albicocco²², J. Albrecht¹⁴, F. Alessio⁴⁷, M. Alexander⁵⁸, A. Alfonso Alberro⁴⁴, G. Alkhazov³⁷, P. Alvarez Cartelle⁶⁰, A.A. Alves Jr⁴⁵, S. Amato², Y. Amhis¹¹, L. An²¹, L. Anderlini²¹, G. Andreassi⁴⁸, M. Andreotti²⁰, F. Archilli¹⁶, J. Arnau Romeu¹⁰, A. Artamonov⁴³, M. Artuso⁶⁷, K. Arzymatov⁴¹, E. Aslanides¹⁰, M. Atzeni⁴⁹, B. Audurier²⁶, S. Bachmann¹⁶, J.J. Back⁵⁵, S. Baker⁶⁰, V. Balagura^{11,b}, W. Baldini^{20,47}, A. Baranov⁴¹, R.J. Barlow⁶¹, S. Barsuk¹¹, W. Barter⁶⁰, M. Bartolini^{23,47,h}, F. Baryshnikov⁷⁷, G. Bassi²⁸, V. Batozskaya³⁵, B. Batsukh⁶⁷, A. Battig¹⁴, A. Bay⁴⁸, M. Becker¹⁴, F. Bedeschi²⁸, I. Bediaga¹, A. Beiter⁶⁷, L.J. Bel³¹, V. Belavin⁴¹, S. Belin²⁶, N. Bely⁵, V. Bellec⁴⁸, K. Belous⁴³, I. Belyaev³⁸, G. Bencivenni²², E. Ben-Haim¹², S. Benson³¹, S. Beranek¹³, A. Berezhnoy³⁹, R. Bernet⁴⁹, D. Berninghoff¹⁶, H.C. Bernstein⁶⁷, C. Bertella⁴⁷, E. Bertholet¹², A. Bertolin²⁷, C. Betancourt⁴⁹, F. Betti^{19,e}, M.O. Bettler⁵⁴, I.a. Bezshyiko⁴⁹, S. Bhasin⁵³, J. Bhom³³, M.S. Bieker¹⁴, S. Bifani⁵², P. Billoir¹², A. Bizzeti^{21,u}, M. Bjørn⁶², M.P. Blago⁴⁷, T. Blake⁵⁵, F. Blanc⁴⁸, S. Blusk⁶⁷, D. Bobulska⁵⁸, V. Bocci³⁰, O. Boente Garcia⁴⁵, T. Boettcher⁶³, A. Boldyrev⁷⁸, A. Bondar^{42,x}, N. Bondar³⁷, S. Borghi^{61,47}, M. Borisyak⁴¹, M. Borsato¹⁶, J.T. Borsuk³³, T.J.V. Bowcock⁵⁹, C. Bozzi²⁰, M.J. Bradley⁶⁰, S. Braun¹⁶, A. Brea Rodriguez⁴⁵, M. Brodski⁴⁷, J. Brodzicka³³, A. Brossa Gonzalo⁵⁵, D. Brundu²⁶, E. Buchanan⁵³, A. Buonauro⁴⁹, C. Burr⁴⁷, A. Bursche²⁶, J.S. Butter³¹, J. Buytaert⁴⁷, W. Byczynski⁴⁷, S. Cadeddu²⁶, H. Cai⁷², R. Calabrese^{20,g}, L. Calero Diaz²², S. Cali²², R. Calladine⁵², M. Calvi^{24,i}, M. Calvo Gomez^{44,m}, P. Camargo Magalhaes⁵³, A. Camboni^{44,m}, P. Campana²², D.H. Campora Perez³¹, L. Capriotti^{19,e}, A. Carbone^{19,e}, G. Carboni²⁹, R. Cardinale^{23,h}, A. Cardini²⁶, P. Carniti^{24,i}, K. Carvalho Akiba³¹, A. Casais Vidal⁴⁵, G. Casse⁵⁹, M. Cattaneo⁴⁷, G. Cavallero⁴⁷, S. Celani⁴⁸, R. Cenci^{28,p}, J. Cerasoli¹⁰, M.G. Chapman⁵³, M. Charles^{12,47}, Ph. Charpentier⁴⁷, G. Chatzikonstantinidis⁵², M. Chefdeville⁸, V. Chekalina⁴¹, C. Chen³, S. Chen²⁶, A. Chernov³³, S.-G. Chitic⁴⁷, V. Chobanova⁴⁵, M. Chrzaszcz³³, A. Chubykin³⁷, P. Ciambrone²², M.F. Cicala⁵⁵, X. Cid Vidal⁴⁵, G. Ciezarek⁴⁷, F. Cindolo¹⁹, P.E.L. Clarke⁵⁷, M. Clemencic⁴⁷, H.V. Cliff⁵⁴, J. Closier⁴⁷, J.L. Cobbledick⁶¹, V. Coco⁴⁷, J.A.B. Coelho¹¹, J. Cogan¹⁰, E. Cogneras⁹, L. Cojocariu³⁶, P. Collins⁴⁷, T. Colombo⁴⁷, A. Comerma-Montells¹⁶, A. Contu²⁶, N. Cooke⁵², G. Coombs⁵⁸, S. Coquereau⁴⁴, G. Corti⁴⁷, C.M. Costa Sobral⁵⁵, B. Couturier⁴⁷, D.C. Craik⁶³, J. Crkovska⁶⁶, A. Crocombe⁵⁵, M. Cruz Torres^{1,ab}, R. Currie⁵⁷, C.L. Da Silva⁶⁶, E. Dall'Occo¹⁴, J. Dalseno^{45,53}, C. D'Ambrosio⁴⁷, A. Danilina³⁸, P. d'Argent¹⁶, A. Davis⁶¹, O. De Aguiar Francisco⁴⁷, K. De Bruyn⁴⁷, S. De Capua⁶¹, M. De Cian⁴⁸, J.M. De Miranda¹, L. De Paula², M. De Serio^{18,d}, P. De Simone²², J.A. de Vries³¹, C.T. Dean⁶⁶, W. Dean⁸⁰, D. Decamp⁸, L. Del Buono¹², B. Delaney⁵⁴, H.-P. Dembinski¹⁵, M. Demmer¹⁴, A. Dendek³⁴, V. Denysenko⁴⁹, D. Derkach⁷⁸, O. Deschamps⁹, F. Desse¹¹, F. Dettori²⁶, B. Dey⁷, A. Di Canto⁴⁷, P. Di Nezza²², S. Didenko⁷⁷, H. Dijkstra⁴⁷, V. Dobishuk⁵¹, F. Dordei²⁶, M. Dorigo^{28,y}, A.C. dos Reis¹, L. Douglas⁵⁸, A. Dovbnya⁵⁰, K. Dreimanis⁵⁹, M.W. Dudek³³, L. Dufour⁴⁷, G. Dujany¹², P. Durante⁴⁷, J.M. Durham⁶⁶, D. Dutta⁶¹, M. Dziewiecki¹⁶, A. Dziurda³³, A. Dzyuba³⁷, S. Easo⁵⁶, U. Egede⁶⁹, V. Egorychev³⁸, S. Eidelman^{42,x}, S. Eisenhardt⁵⁷, R. Ekelhof¹⁴, S. Ek-In⁴⁸, L. Eklund⁵⁸, S. Ely⁶⁷, A. Ene³⁶, E. Eppe⁶⁶, S. Escher¹³, S. Esen³¹, T. Evans⁴⁷, A. Falabella¹⁹, J. Fan³, N. Farley⁵², S. Farry⁵⁹, D. Fazzini¹¹, P. Fedin³⁸, M. Féo⁴⁷, P. Fernandez Declara⁴⁷, A. Fernandez Prieto⁴⁵, F. Ferrari^{19,e}, L. Ferreira Lopes⁴⁸, F. Ferreira Rodrigues², S. Ferreres Sole³¹, M. Ferrillo⁴⁹, M. Ferro-Luzzi⁴⁷, S. Filippov⁴⁰, R.A. Fini¹⁸, M. Fiorini^{20,g}, M. Firlej³⁴, K.M. Fischer⁶², C. Fitzpatrick⁴⁷, T. Fiutowski³⁴, F. Fleuret^{11,b}, M. Fontana⁴⁷, F. Fontanelli^{23,h}, R. Forty⁴⁷, V. Franco Lima⁵⁹, M. Franco Sevilla⁶⁵, M. Frank⁴⁷, C. Frei⁴⁷, D.A. Friday⁵⁸, J. Fu^{25,q}, M. Fuehring¹⁴, W. Funk⁴⁷, E. Gabriel⁵⁷, A. Gallas Torreira⁴⁵, D. Galli^{19,e}, S. Gallorini²⁷, S. Gambetta⁵⁷, Y. Gan³, M. Gandelman², P. Gandini²⁵, Y. Gao⁴, L.M. Garcia Martin⁴⁶, J. García Pardiñas⁴⁹,

B. Garcia Plana⁴⁵, F.A. Garcia Rosales¹¹, J. Garra Tico⁵⁴, L. Garrido⁴⁴, D. Gascon⁴⁴,
 C. Gaspar⁴⁷, D. Gerick¹⁶, E. Gersabeck⁶¹, M. Gersabeck⁶¹, T. Gershon⁵⁵, D. Gerstel¹⁰,
 Ph. Ghez⁸, V. Gibson⁵⁴, A. Gioventù⁴⁵, O.G. Girard⁴⁸, P. Gironella Gironell⁴⁴, L. Giubega³⁶,
 C. Giugliano²⁰, K. Gizdov⁵⁷, V.V. Gligorov¹², C. Göbel⁷⁰, D. Golubkov³⁸, A. Golutvin^{60,77},
 A. Gomes^{1,a}, P. Gorbounov^{38,6}, I.V. Gorelov³⁹, C. Gotti^{24,i}, E. Govorkova³¹, J.P. Grabowski¹⁶,
 R. Graciani Diaz⁴⁴, T. Grammatico¹², L.A. Granado Cardoso⁴⁷, E. Graugés⁴⁴, E. Graverini⁴⁸,
 G. Graziani²¹, A. Grecu³⁶, R. Greim³¹, P. Griffith²⁰, L. Grillo⁶¹, L. Gruber⁴⁷,
 B.R. Gruberg Cazon⁶², C. Gu³, E. Gushchin⁴⁰, A. Guth¹³, Yu. Guz^{43,47}, T. Gys⁴⁷, P. Gnther¹⁶,
 T. Hadavizadeh⁶², G. Haefeli⁴⁸, C. Haen⁴⁷, S.C. Haines⁵⁴, P.M. Hamilton⁶⁵, Q. Han⁷, X. Han¹⁶,
 T.H. Hancock⁶², S. Hansmann-Menzemer¹⁶, N. Harnew⁶², T. Harrison⁵⁹, R. Hart³¹, C. Hasse⁴⁷,
 M. Hatch⁴⁷, J. He⁵, M. Hecker⁶⁰, K. Heijhoff³¹, K. Heinicke¹⁴, A. Heister¹⁴, A.M. Hennequin⁴⁷,
 K. Hennessy⁵⁹, L. Henry⁴⁶, J. Heuel¹³, A. Hicheur⁶⁸, D. Hill⁶², M. Hilton⁶¹, P.H. Hopchev⁴⁸,
 J. Hu¹⁶, W. Hu⁷, W. Huang⁵, W. Hulsbergen³¹, T. Humair⁶⁰, R.J. Hunter⁵⁵, M. Hushchyn⁷⁸,
 D. Hutchcroft⁵⁹, D. Hynds³¹, P. Ibis¹⁴, M. Idzik³⁴, P. Ilten⁵², A. Inglezzi³⁷, A. Inyakin⁴³,
 K. Ivshin³⁷, R. Jacobsson⁴⁷, S. Jakobsen⁴⁷, E. Jans³¹, B.K. Jashal⁴⁶, A. Jawahery⁶⁵,
 V. Jevtic¹⁴, F. Jiang³, M. John⁶², D. Johnson⁴⁷, C.R. Jones⁵⁴, B. Jost⁴⁷, N. Jurik⁶²,
 S. Kandybei⁵⁰, M. Karacson⁴⁷, J.M. Kariuki⁵³, N. Kazeev⁷⁸, M. Kecke¹⁶, F. Keizer^{54,54},
 M. Kelsey⁶⁷, M. Kenzie⁵⁵, T. Ketel³², B. Khanji⁴⁷, A. Kharisova⁷⁹, K.E. Kim⁶⁷, T. Kirn¹³,
 V.S. Kirsbaum⁴⁸, S. Klaver²², K. Klimaszewski³⁵, S. Koliiev⁵¹, A. Kondybayeva⁷⁷,
 A. Konoplyannikov³⁸, P. Kopciwicz³⁴, R. Kopečna¹⁶, P. Koppenburg³¹, I. Kostiuk^{31,51},
 O. Kot⁵¹, S. Kotriakhova³⁷, L. Kravchuk⁴⁰, R.D. Krawczyk⁴⁷, M. Kreps⁵⁵, F. Kress⁶⁰,
 S. Kretschmar¹³, P. Krokovny^{42,x}, W. Krupa³⁴, W. Krzemien³⁵, W. Kucewicz^{33,l},
 M. Kucharczyk³³, V. Kudryavtsev^{42,x}, H.S. Kuindersma³¹, G.J. Kunde⁶⁶, T. Kvaratskheliya³⁸,
 D. Lacarrere⁴⁷, G. Lafferty⁶¹, A. Lai²⁶, D. Lancierini⁴⁹, J.J. Lane⁶¹, G. Lanfranchi²²,
 C. Langenbruch¹³, O. Lantwin⁴⁹, T. Latham⁵⁵, F. Lazzari^{28,v}, C. Lazzeroni⁵², R. Le Gac¹⁰,
 R. Lefèvre⁹, A. Leflat³⁹, O. Leroy¹⁰, T. Lesiak³³, B. Leverington¹⁶, H. Li⁷¹, X. Li⁶⁶, Y. Li⁶,
 Z. Li⁶⁷, X. Liang⁶⁷, R. Lindner⁴⁷, V. Lisovskyi¹⁴, G. Liu⁷¹, X. Liu³, D. Loh⁵⁵, A. Loi²⁶,
 J. Lomba Castro⁴⁵, I. Longstaff⁵⁸, J.H. Lopes², G. Loustau⁴⁹, G.H. Lovell⁵⁴, Y. Lu⁶,
 D. Lucchesi^{27,o}, M. Lucio Martinez³¹, Y. Luo³, A. Lupato²⁷, E. Luppi^{20,g}, O. Lupton⁵⁵,
 A. Lusiani^{28,t}, X. Lyu⁵, S. Maccolini^{19,e}, F. Machefer¹¹, F. Maciuc³⁶, V. Macko⁴⁸,
 P. Mackowiak¹⁴, S. Maddrell-Mander⁵³, L.R. Madhan Mohan⁵³, O. Maev^{37,47}, A. Maevskiy⁷⁸,
 D. Maisuzenko³⁷, M.W. Majewski³⁴, S. Malde⁶², B. Malecki⁴⁷, A. Malinin⁷⁶, T. Maltsev^{42,x},
 H. Malygina¹⁶, G. Manca^{26,f}, G. Mancinelli¹⁰, R. Manera Escalero⁴⁴, D. Manuzzi^{19,e},
 D. Marangotto^{25,q}, J. Maratas^{9,w}, J.F. Marchand⁸, U. Marconi¹⁹, S. Mariani²¹,
 C. Marin Benito¹¹, M. Marinangeli⁴⁸, P. Marino⁴⁸, J. Marks¹⁶, P.J. Marshall⁵⁹, G. Martellotti³⁰,
 L. Martinazzoli⁴⁷, M. Martinelli^{24,i}, D. Martinez Santos⁴⁵, F. Martinez Vidal⁴⁶, A. Massafferri¹,
 M. Materok¹³, R. Matev⁴⁷, A. Mathad⁴⁹, Z. Mathe⁴⁷, V. Matiunin³⁸, C. Matteuzzi²⁴,
 K.R. Mattioli⁸⁰, A. Mauri⁴⁹, E. Maurice^{11,b}, M. McCann⁶⁰, L. McConnell¹⁷, A. McNab⁶¹,
 R. McNulty¹⁷, J.V. Mead⁵⁹, B. Meadows⁶⁴, C. Meaux¹⁰, G. Meier¹⁴, N. Meinert⁷⁴,
 D. Melnychuk³⁵, S. Meloni^{24,i}, M. Merk³¹, A. Merli²⁵, M. Mikhasenko⁴⁷, D.A. Milanese⁷³,
 E. Millard⁵⁵, M.-N. Minard⁸, O. Mineev³⁸, L. Minzoni^{20,g}, S.E. Mitchell⁵⁷, B. Mitreska⁶¹,
 D.S. Mitzel⁴⁷, A. Mödden¹⁴, A. Mogini¹², R.D. Moise⁶⁰, T. Mombächer¹⁴, I.A. Monroy⁷³,
 S. Monteil⁹, M. Morandin²⁷, G. Morello²², M.J. Morello^{28,t}, J. Moron³⁴, A.B. Morris¹⁰,
 A.G. Morris⁵⁵, R. Mountain⁶⁷, H. Mu³, F. Muheim⁵⁷, M. Mukherjee⁷, M. Mulder³¹,
 D. Müller⁴⁷, K. Müller⁴⁹, V. Müller¹⁴, C.H. Murphy⁶², D. Murray⁶¹, P. Muzzetto²⁶, P. Naik⁵³,
 T. Nakada⁴⁸, R. Nandakumar⁵⁶, A. Nandi⁶², T. Nanut⁴⁸, I. Nasteva², M. Needham⁵⁷,
 N. Neri^{25,q}, S. Neubert¹⁶, N. Neufeld⁴⁷, R. Newcombe⁶⁰, T.D. Nguyen⁴⁸, C. Nguyen-Mau^{48,n},
 E.M. Niel¹¹, S. Nieswand¹³, N. Nikitin³⁹, N.S. Nolte⁴⁷, C. Nunez⁸⁰, A. Oblakowska-Mucha³⁴,
 V. Obraztsov⁴³, S. Ogilvy⁵⁸, D.P. O’Hanlon¹⁹, R. Oldeman^{26,f}, C.J.G. Onderwater⁷⁵, J.
 D. Osborn⁸⁰, A. Ossowska³³, J.M. Otalora Goicochea², T. Ovsiannikova³⁸, P. Owen⁴⁹,

A. Oyanguren⁴⁶, P.R. Pais⁴⁸, T. Pajero^{28,t}, A. Palano¹⁸, M. Palutan²², G. Panshin⁷⁹,
 A. Papanestis⁵⁶, M. Pappagallo⁵⁷, L.L. Pappalardo^{20,g}, C. Pappenheimer⁶⁴, W. Parker⁶⁵,
 C. Parkes⁶¹, G. Passaleva^{21,47}, A. Pastore¹⁸, M. Patel⁶⁰, C. Patrignani^{19,e}, A. Pearce⁴⁷,
 A. Pellegrino³¹, M. Pepe Altarelli⁴⁷, S. Perazzini¹⁹, D. Pereima³⁸, P. Perret⁹, L. Pescatore⁴⁸,
 K. Petridis⁵³, A. Petrolini^{23,h}, A. Petrov⁷⁶, S. Petrucci⁵⁷, M. Petruzzo^{25,q}, B. Pietrzyk⁸,
 G. Pietrzyk⁴⁸, M. Pili⁶², D. Pinci³⁰, J. Pinzino⁴⁷, F. Pisani⁴⁷, A. Piucci¹⁶, V. Placinta³⁶,
 S. Playfer⁵⁷, J. Plews⁵², M. Plo Casasus⁴⁵, F. Polci¹², M. Poli Lener²², M. Poliakov⁶⁷,
 A. Poluektov¹⁰, N. Polukhina^{77,c}, I. Polyakov⁶⁷, E. Polycarpo², G.J. Pomery⁵³, S. Ponce⁴⁷,
 A. Popov⁴³, D. Popov⁵², S. Poslavskii⁴³, K. Prasanth³³, L. Promberger⁴⁷, C. Prouve⁴⁵,
 V. Pugatch⁵¹, A. Puig Navarro⁴⁹, H. Pullen⁶², G. Punzi^{28,p}, W. Qian⁵, J. Qin⁵, R. Quagliani¹²,
 B. Quintana⁹, N.V. Raab¹⁷, R.I. Rabadan Trejo¹⁰, B. Rachwal³⁴, J.H. Rademacker⁵³,
 M. Rama²⁸, M. Ramos Pernas⁴⁵, M.S. Rangel², F. Ratnikov^{41,78}, G. Raven³², M. Reboud⁸,
 F. Redi⁴⁸, F. Reiss¹², C. Remon Alepuz⁴⁶, Z. Ren³, V. Renaudin⁶², S. Ricciardi⁵⁶,
 S. Richards⁵³, K. Rinnert⁵⁹, P. Robbe¹¹, A. Robert¹², A.B. Rodrigues⁴⁸, E. Rodrigues⁶⁴,
 J.A. Rodriguez Lopez⁷³, M. Roehrken⁴⁷, S. Roiser⁴⁷, A. Rollings⁶², V. Romanovskiy⁴³,
 M. Romero Lamas⁴⁵, A. Romero Vidal⁴⁵, J.D. Roth⁸⁰, M. Rotondo²², M.S. Rudolph⁶⁷,
 T. Ruf⁴⁷, J. Ruiz Vidal⁴⁶, J. Ryzka³⁴, J.J. Saborido Silva⁴⁵, N. Sagidova³⁷, B. Saitta^{26,f},
 C. Sanchez Gras³¹, C. Sanchez Mayordomo⁴⁶, R. Santacesaria³⁰, C. Santamarina Rios⁴⁵,
 M. Santimaria²², E. Santovetti^{29,j}, G. Sarpis⁶¹, A. Sarti³⁰, C. Satriano^{30,s}, A. Satta²⁹, M. Saur⁵,
 D. Savrina^{38,39}, L.G. Scantlebury Smead⁶², S. Schael¹³, M. Schellenberg¹⁴, M. Schiller⁵⁸,
 H. Schindler⁴⁷, M. Schmelling¹⁵, T. Schmelzer¹⁴, B. Schmidt⁴⁷, O. Schneider⁴⁸, A. Schopper⁴⁷,
 H.F. Schreiner⁶⁴, M. Schubiger³¹, S. Schulte⁴⁸, M.H. Schune¹¹, R. Schwemmer⁴⁷, B. Sciascia²²,
 A. Sciubba^{30,k}, S. Sellam⁶⁸, A. Semennikov³⁸, A. Sergi^{52,47}, N. Serra⁴⁹, J. Serrano¹⁰,
 L. Sestini²⁷, A. Seuthe¹⁴, P. Seyfert⁴⁷, D.M. Shangase⁸⁰, M. Shapkin⁴³, L. Shchutska⁴⁸,
 T. Shears⁵⁹, L. Shekhtman^{42,x}, V. Shevchenko^{76,77}, E. Shmanin⁷⁷, J.D. Shupperd⁶⁷,
 B.G. Siddi²⁰, R. Silva Coutinho⁴⁹, L. Silva de Oliveira², G. Simi^{27,o}, S. Simone^{18,d}, I. Skiba²⁰,
 N. Skidmore¹⁶, T. Skwarnicki⁶⁷, M.W. Slater⁵², J.G. Smeaton⁵⁴, A. Smetkina³⁸, E. Smith¹³,
 I.T. Smith⁵⁷, M. Smith⁶⁰, A. Snoch³¹, M. Soares¹⁹, L. Soares Lavoura¹, M.D. Sokoloff⁶⁴,
 F.J.P. Soler⁵⁸, B. Souza De Paula², B. Spaan¹⁴, E. Spadaro Norella^{25,q}, P. Spradlin⁵⁸,
 F. Stagni⁴⁷, M. Stahl⁶⁴, S. Stahl⁴⁷, P. Stefko⁴⁸, O. Steinkamp⁴⁹, S. Stemmler¹⁶, O. Stenyakin⁴³,
 M. Stepanova³⁷, H. Stevens¹⁴, S. Stone⁶⁷, S. Stracka²⁸, M.E. Stramaglia⁴⁸, M. Straticiu³⁶,
 S. Strokov⁷⁹, J. Sun³, L. Sun⁷², Y. Sun⁶⁵, P. Svihra⁶¹, K. Swientek³⁴, A. Szabelski³⁵,
 T. Szumlak³⁴, M. Szymanski⁵, S. Taneja⁶¹, Z. Tang³, T. Tekampe¹⁴, G. Tellarini²⁰,
 F. Teubert⁴⁷, E. Thomas⁴⁷, K.A. Thomson⁵⁹, M.J. Tilley⁶⁰, V. Tisserand⁹, S. T'Jampens⁸,
 M. Tobin⁶, S. Tolk⁴⁷, L. Tomassetti^{20,g}, D. Tonelli²⁸, D. Torres Machado¹, D.Y. Tou¹²,
 E. Tournefier⁸, M. Traill⁵⁸, M.T. Tran⁴⁸, C. Trippl⁴⁸, A. Trisovic⁵⁴, A. Tsaregorodtsev¹⁰,
 G. Tuci^{28,47,p}, A. Tully⁴⁸, N. Tuning³¹, A. Ukleja³⁵, A. Usachov¹¹, A. Ustyuzhanin^{41,78},
 U. Uwer¹⁶, A. Vagner⁷⁹, V. Vagnoni¹⁹, A. Valassi⁴⁷, G. Valenti¹⁹, M. van Beuzekom³¹,
 H. Van Hecke⁶⁶, E. van Herwijnen⁴⁷, C.B. Van Hulse¹⁷, M. van Veghel⁷⁵, R. Vazquez Gomez⁴⁴,
 P. Vazquez Regueiro⁴⁵, C. Vázquez Sierra³¹, S. Vecchi²⁰, J.J. Velthuis⁵³, M. Veltri^{21,r},
 A. Venkateswaran⁶⁷, M. Vernet⁹, M. Veronesi³¹, M. Vesterinen⁵⁵, J.V. Viana Barbosa⁴⁷,
 D. Vieira⁵, M. Vieites Diaz⁴⁸, H. Viemann⁷⁴, X. Vilasis-Cardona^{44,m}, A. Vitkovskiy³¹,
 V. Volkov³⁹, A. Vollhardt⁴⁹, D. Vom Bruch¹², A. Vorobyev³⁷, V. Vorobyev^{42,x}, N. Voropaev³⁷,
 R. Waldi⁷⁴, J. Walsh²⁸, J. Wang³, J. Wang⁷², J. Wang⁶, M. Wang³, Y. Wang⁷, Z. Wang⁴⁹,
 D.R. Ward⁵⁴, H.M. Wark⁵⁹, N.K. Watson⁵², D. Websdale⁶⁰, A. Weiden⁴⁹, C. Weisser⁶³,
 B.D.C. Westhenry⁵³, D.J. White⁶¹, M. Whitehead¹³, D. Wiedner¹⁴, G. Wilkinson⁶²,
 M. Wilkinson⁶⁷, I. Williams⁵⁴, M. Williams⁶³, M.R.J. Williams⁶¹, T. Williams⁵², F.F. Wilson⁵⁶,
 W. Wislicki³⁵, M. Witek³³, L. Witola¹⁶, G. Wormser¹¹, S.A. Wotton⁵⁴, H. Wu⁶⁷, K. Wyllie⁴⁷,
 Z. Xiang⁵, D. Xiao⁷, Y. Xie⁷, H. Xing⁷¹, A. Xu³, L. Xu³, M. Xu⁷, Q. Xu⁵, Z. Xu⁸, Z. Xu⁴,
 Z. Yang³, Z. Yang⁶⁵, Y. Yao⁶⁷, L.E. Yeomans⁵⁹, H. Yin⁷, J. Yu^{7,aa}, X. Yuan⁶⁷,

O. Yushchenko⁴³, K.A. Zarebski⁵², M. Zavertyaev^{15,c}, M. Zdybal³³, M. Zeng³, D. Zhang⁷, L. Zhang³, S. Zhang³, W.C. Zhang^{3,z}, Y. Zhang⁴⁷, A. Zhelezov¹⁶, Y. Zheng⁵, X. Zhou⁵, Y. Zhou⁵, X. Zhu³, V. Zhukov^{13,39}, J.B. Zonneveld⁵⁷, S. Zucchelli^{19,e}.

¹*Centro Brasileiro de Pesquisas Físicas (CBPF), Rio de Janeiro, Brazil*

²*Universidade Federal do Rio de Janeiro (UFRJ), Rio de Janeiro, Brazil*

³*Center for High Energy Physics, Tsinghua University, Beijing, China*

⁴*School of Physics State Key Laboratory of Nuclear Physics and Technology, Peking University, Beijing, China*

⁵*University of Chinese Academy of Sciences, Beijing, China*

⁶*Institute Of High Energy Physics (IHEP), Beijing, China*

⁷*Institute of Particle Physics, Central China Normal University, Wuhan, Hubei, China*

⁸*Univ. Grenoble Alpes, Univ. Savoie Mont Blanc, CNRS, IN2P3-LAPP, Annecy, France*

⁹*Université Clermont Auvergne, CNRS/IN2P3, LPC, Clermont-Ferrand, France*

¹⁰*Aix Marseille Univ, CNRS/IN2P3, CPPM, Marseille, France*

¹¹*LAL, Univ. Paris-Sud, CNRS/IN2P3, Université Paris-Saclay, Orsay, France*

¹²*LPNHE, Sorbonne Université, Paris Diderot Sorbonne Paris Cité, CNRS/IN2P3, Paris, France*

¹³*I. Physikalisches Institut, RWTH Aachen University, Aachen, Germany*

¹⁴*Fakultät Physik, Technische Universität Dortmund, Dortmund, Germany*

¹⁵*Max-Planck-Institut für Kernphysik (MPIK), Heidelberg, Germany*

¹⁶*Physikalisches Institut, Ruprecht-Karls-Universität Heidelberg, Heidelberg, Germany*

¹⁷*School of Physics, University College Dublin, Dublin, Ireland*

¹⁸*INFN Sezione di Bari, Bari, Italy*

¹⁹*INFN Sezione di Bologna, Bologna, Italy*

²⁰*INFN Sezione di Ferrara, Ferrara, Italy*

²¹*INFN Sezione di Firenze, Firenze, Italy*

²²*INFN Laboratori Nazionali di Frascati, Frascati, Italy*

²³*INFN Sezione di Genova, Genova, Italy*

²⁴*INFN Sezione di Milano-Bicocca, Milano, Italy*

²⁵*INFN Sezione di Milano, Milano, Italy*

²⁶*INFN Sezione di Cagliari, Monserrato, Italy*

²⁷*INFN Sezione di Padova, Padova, Italy*

²⁸*INFN Sezione di Pisa, Pisa, Italy*

²⁹*INFN Sezione di Roma Tor Vergata, Roma, Italy*

³⁰*INFN Sezione di Roma La Sapienza, Roma, Italy*

³¹*Nikhef National Institute for Subatomic Physics, Amsterdam, Netherlands*

³²*Nikhef National Institute for Subatomic Physics and VU University Amsterdam, Amsterdam, Netherlands*

³³*Henryk Niewodniczanski Institute of Nuclear Physics Polish Academy of Sciences, Kraków, Poland*

³⁴*AGH - University of Science and Technology, Faculty of Physics and Applied Computer Science, Kraków, Poland*

³⁵*National Center for Nuclear Research (NCBJ), Warsaw, Poland*

³⁶*Horia Hulubei National Institute of Physics and Nuclear Engineering, Bucharest-Magurele, Romania*

³⁷*Petersburg Nuclear Physics Institute NRC Kurchatov Institute (PNPI NRC KI), Gatchina, Russia*

³⁸*Institute of Theoretical and Experimental Physics NRC Kurchatov Institute (ITEP NRC KI), Moscow, Russia, Moscow, Russia*

³⁹*Institute of Nuclear Physics, Moscow State University (SINP MSU), Moscow, Russia*

⁴⁰*Institute for Nuclear Research of the Russian Academy of Sciences (INR RAS), Moscow, Russia*

⁴¹*Yandex School of Data Analysis, Moscow, Russia*

⁴²*Budker Institute of Nuclear Physics (SB RAS), Novosibirsk, Russia*

⁴³*Institute for High Energy Physics NRC Kurchatov Institute (IHEP NRC KI), Protvino, Russia, Protvino, Russia*

⁴⁴*ICCUB, Universitat de Barcelona, Barcelona, Spain*

⁴⁵*Instituto Galego de Física de Altas Enerxías (IGFAE), Universidade de Santiago de Compostela, Santiago de Compostela, Spain*

⁴⁶*Instituto de Física Corpuscular, Centro Mixto Universidad de Valencia - CSIC, Valencia, Spain*

- ⁴⁷ *European Organization for Nuclear Research (CERN), Geneva, Switzerland*
- ⁴⁸ *Institute of Physics, Ecole Polytechnique Fédérale de Lausanne (EPFL), Lausanne, Switzerland*
- ⁴⁹ *Physik-Institut, Universität Zürich, Zürich, Switzerland*
- ⁵⁰ *NSC Kharkiv Institute of Physics and Technology (NSC KIPT), Kharkiv, Ukraine*
- ⁵¹ *Institute for Nuclear Research of the National Academy of Sciences (KINR), Kyiv, Ukraine*
- ⁵² *University of Birmingham, Birmingham, United Kingdom*
- ⁵³ *H.H. Wills Physics Laboratory, University of Bristol, Bristol, United Kingdom*
- ⁵⁴ *Cavendish Laboratory, University of Cambridge, Cambridge, United Kingdom*
- ⁵⁵ *Department of Physics, University of Warwick, Coventry, United Kingdom*
- ⁵⁶ *STFC Rutherford Appleton Laboratory, Didcot, United Kingdom*
- ⁵⁷ *School of Physics and Astronomy, University of Edinburgh, Edinburgh, United Kingdom*
- ⁵⁸ *School of Physics and Astronomy, University of Glasgow, Glasgow, United Kingdom*
- ⁵⁹ *Oliver Lodge Laboratory, University of Liverpool, Liverpool, United Kingdom*
- ⁶⁰ *Imperial College London, London, United Kingdom*
- ⁶¹ *Department of Physics and Astronomy, University of Manchester, Manchester, United Kingdom*
- ⁶² *Department of Physics, University of Oxford, Oxford, United Kingdom*
- ⁶³ *Massachusetts Institute of Technology, Cambridge, MA, United States*
- ⁶⁴ *University of Cincinnati, Cincinnati, OH, United States*
- ⁶⁵ *University of Maryland, College Park, MD, United States*
- ⁶⁶ *Los Alamos National Laboratory (LANL), Los Alamos, United States*
- ⁶⁷ *Syracuse University, Syracuse, NY, United States*
- ⁶⁸ *Laboratory of Mathematical and Subatomic Physics , Constantine, Algeria, associated to ²*
- ⁶⁹ *School of Physics and Astronomy, Monash University, Melbourne, Australia, associated to ⁵⁵*
- ⁷⁰ *Pontifícia Universidade Católica do Rio de Janeiro (PUC-Rio), Rio de Janeiro, Brazil, associated to ²*
- ⁷¹ *South China Normal University, Guangzhou, China, associated to ³*
- ⁷² *School of Physics and Technology, Wuhan University, Wuhan, China, associated to ³*
- ⁷³ *Departamento de Física , Universidad Nacional de Colombia, Bogota, Colombia, associated to ¹²*
- ⁷⁴ *Institut für Physik, Universität Rostock, Rostock, Germany, associated to ¹⁶*
- ⁷⁵ *Van Swinderen Institute, University of Groningen, Groningen, Netherlands, associated to ³¹*
- ⁷⁶ *National Research Centre Kurchatov Institute, Moscow, Russia, associated to ³⁸*
- ⁷⁷ *National University of Science and Technology “MISIS”, Moscow, Russia, associated to ³⁸*
- ⁷⁸ *National Research University Higher School of Economics, Moscow, Russia, associated to ⁴¹*
- ⁷⁹ *National Research Tomsk Polytechnic University, Tomsk, Russia, associated to ³⁸*
- ⁸⁰ *University of Michigan, Ann Arbor, United States, associated to ⁶⁷*

^a *Universidade Federal do Triângulo Mineiro (UFTM), Uberaba-MG, Brazil*

^b *Laboratoire Leprince-Ringuet, Palaiseau, France*

^c *P.N. Lebedev Physical Institute, Russian Academy of Science (LPI RAS), Moscow, Russia*

^d *Università di Bari, Bari, Italy*

^e *Università di Bologna, Bologna, Italy*

^f *Università di Cagliari, Cagliari, Italy*

^g *Università di Ferrara, Ferrara, Italy*

^h *Università di Genova, Genova, Italy*

ⁱ *Università di Milano Bicocca, Milano, Italy*

^j *Università di Roma Tor Vergata, Roma, Italy*

^k *Università di Roma La Sapienza, Roma, Italy*

^l *AGH - University of Science and Technology, Faculty of Computer Science, Electronics and Telecommunications, Kraków, Poland*

^m *DS4DS, La Salle, Universitat Ramon Llull, Barcelona, Spain*

ⁿ *Hanoi University of Science, Hanoi, Vietnam*

^o *Università di Padova, Padova, Italy*

^p *Università di Pisa, Pisa, Italy*

^q *Università degli Studi di Milano, Milano, Italy*

^r *Università di Urbino, Urbino, Italy*

^s *Università della Basilicata, Potenza, Italy*

^t *Scuola Normale Superiore, Pisa, Italy*

^u *Università di Modena e Reggio Emilia, Modena, Italy*

^v *Università di Siena, Siena, Italy*

^w *MSU - Iligan Institute of Technology (MSU-IIT), Iligan, Philippines*

^x *Novosibirsk State University, Novosibirsk, Russia*

^y *INFN Sezione di Trieste, Trieste, Italy*

^z *School of Physics and Information Technology, Shaanxi Normal University (SNNU), Xi'an, China*

^{aa} *Physics and Micro Electronic College, Hunan University, Changsha City, China*

^{ab} *Universidad Nacional Autonoma de Honduras, Tegucigalpa, Honduras*

[†] *Deceased*